



Curso Académico 2022/23

TRABAJO FINAL DE MÁSTER

---

**THE ROLE OF ZONULIN IN GLIOBLASTOMA BIOLOGY**

---

**Roberta Repossi**

Tutorizado por:

**Prof. Julio Manuel Plata Bello**

**PhD. Rita Marleny Martín Ramírez**

Grupo de investigación:

**Neurociencia Clínica**

Dr. **Julio Manuel Plata Bello**, profesor asociado del Departamento de Enfermería de la Universidad de La Laguna (ULL), integrado en la línea de investigación “Neurociencia clínica” del Instituto de Tecnologías Biomédicas (ITB) y adscrito a las líneas de investigación incluidas en la titulación “Máster en Biomedicina” y la Dra. **Rita Marleny Martín Ramírez**, investigadora colaboradora del grupo de investigación “Biología del Desarrollo” del Departamento de Bioquímica, Biología celular, Microbiología y Genética de la ULL, en calidad de tutor y co-tutora

CERTIFICAN:

- Que el Trabajo Final de Máster (TFM) titulado “The role of zonulin in Glioblastoma biology” ha sido realizado bajo nuestra supervisión por la alumna Roberta Reposi, durante el curso académico 2022/2023.
- Que una vez revisada la memoria final del TFM, damos nuestro consentimiento para ser presentada a la evaluación (lectura y defensa) por el tribunal asignado por la Comisión Académica del Máster en Biomedicina.

Para que conste y surta los efectos oportunos, firman la presente en La Laguna a 05 de julio de 2023, el tutor y la co-tutora.

C/ Padre Herrera s/n  
38207 La Laguna  
Santa Cruz de Tenerife. España

T: 900 43 25 26

[ull.es](http://ull.es)

Este documento incorpora firma electrónica, y es copia auténtica de un documento electrónico archivado por la ULL según la Ley 39/2015.  
*La autenticidad de este documento puede ser comprobada en la dirección: <http://sede.ull.es/validacion>*

Identificador del documento: 5606981 Código de verificación: lcXxcvIv

Firmado por: Rita Marleny Martín Ramírez  
UNIVERSIDAD DE LA LAGUNA

Fecha: 05/07/2023 15:01:02

Julio Manuel Plata Bello  
UNIVERSIDAD DE LA LAGUNA

05/07/2023 15:20:40

## INDEX

ABSTRACT-----	5
RESUMEN -----	6
INTRODUCTION-----	7
Glioblastoma (GB) -----	7
Blood brain barrier (BBB) impairment in GB -----	8
Zonulin-----	9
Zonulin in GB -----	11
MATERIALS AND METHODS-----	15
GB patients -----	15
Tissue collection -----	15
Cell lines and cell culture-----	16
Neurosphere induction from U-87MG cell line-----	16
RNA extraction and cDNA synthesis -----	17
Quantitative real-time polymerase chain reaction (qRT-PCR) -----	18
Western Blot-----	19
Immunocytochemistry (ICC)-----	21
Enzyme-linked immunosorbent assay (ELISA) -----	22
Image analysis-----	23
Statistical analysis -----	23
RESULTS -----	25
Analysis of zonulin and haptoglobin expression in patient serum -----	25
Analysis of zonulin expression in patient tumour samples-----	26
Analysis of zonulin expression in U-87MG and U-118MG cell lines -----	32
Analysis of neurosphere development and characterization -----	33

Analysis of zonulin expression in neurospheres -----	36
Comparison of zonulin expression among tumour samples, glioma cell lines and neurospheres-----	38
DISCUSSION-----	40
Zonulin expression in cell lines increased in stemness conditions -----	40
Tumour samples showed an intermediate expression of zonulin compared to glioma cell lines and neurospheres. -----	41
Zonulin expression in patients was associated with clinical features -----	42
Future perspectives -----	43
CONCLUSIONS -----	44
BIBLIOGRAPHY -----	45

## ABSTRACT

**Background:** Glioblastoma (GB) is one of the most malignant and widespread primary brain tumours. Cerebral oedema is a seriously associated clinical feature, mainly due to blood brain barrier (BBB) impairment and correlated with a worse prognosis. Moreover, glioma stem cells (GSCs) in GB contribute to symptoms aggravation and treatment resistance. Zonulin, a molecule implicated in endothelial tight junction disengagement in BBB, is overexpressed in serum of high-grade glioma patients and in an *in vitro* BBB model submitted to invasiveness assay. **Methods:** To assess a possible implication of zonulin in BBB impairment and tumour progression in GB, zonulin expression was analysed in patients (tumoral tissue and serum), glioma cell lines U-87MG and U-118MG, and GSCs *in vitro* (neurospheres). Both mRNA and protein expression were quantified, using quantitative real-time polymerase-chain-reaction and western blot, respectively, and zonulin cellular location was detected by immunofluorescence. Then, zonulin levels were correlated to clinical parameters. **Results:** Zonulin protein, mainly located in nuclei, was expressed in tumoral samples, at an intermediate level between neurospheres (highest) and glioma cell lines (lowest) ( $p=0.010$ ). Moreover, zonulin was correlated to oedema volume ( $p=0.037$ ) and contrast enhancement volume ( $p=0.020$ ), and its serum levels were associated to a worse prognosis ( $p=0.012$ ). **Conclusions:** In patients, high levels of zonulin are associated with some clinical parameters, as oedema volume, contrast enhancement volume and survival outcomes; in patients, zonulin is more expressed than in glioma cell lines; GSCs *in vitro* express elevated levels of zonulin.

## RESUMEN

**Antecedentes:** El glioblastoma (GB) es uno de los tumores cerebrales primarios más malignos y difusos. El edema cerebral, debido a la disrupción de la barrera hematoencefálica (BHE), constituye un grave efecto adverso y se correlaciona con un peor pronóstico. Las células estaminales de glioma (CEG) contribuyen a la resistencia a los tratamientos. La zonulina, una molécula involucrada en el desensamble de las uniones estrechas del endotelio de la BHE, se sobre expresa en el suero de pacientes con glioma de alto grado y en un modelo de BHE sometido a un ensayo de invasividad. **Métodos:** Para determinar una posible implicación de la zonulina en la disfunción de la BHE y en la progresión tumoral en GB, su expresión (ARN y proteína) se cuantificó en pacientes (tejidos tumorales y suero), líneas celulares de glioma U-87MG y U-118MG, y CEG *in vitro* (neuroesferas). A continuación, se realizó un análisis de correlación con los parámetros clínicos. Además, se determinó su localización celular con inmunofluorescencia. **Resultados:** Los pacientes mostraban una expresión de zonulina intermedia entre las neuroesferas (mayor) y las líneas celulares de glioma (menor) ( $p=0.010$ ). En las muestras tumorales la zonulina se correlacionaba con el volumen de edema y de captación de contraste, y sus niveles séricos a un peor pronóstico. **Conclusiones:** En pacientes, los niveles de zonulina se asocian a volumen de edema, captación de contraste y prognosis; en pacientes, la zonulina se expresa más que en las líneas celulares de glioma; las CEG *in vitro* expresan elevados niveles de zonulina.

## INTRODUCTION

### **Glioblastoma (GB)**

Glioblastoma (GB) represents the most common and aggressive primary brain tumour in adults (mean onset age: 65 years), with an annual incidence of approximately 3/100,000 and being males more affected than females. Around 90% of GBs are diagnosed as *de novo* tumours, and typically show epidermal growth factor receptor (EGFR) overexpression, while the smaller percentage of secondary GBs (mean age: 45 years) develop from lower-grade gliomas that acquire additional individual mutations<sup>1</sup>. GB shows a high heterogeneity and malignancy at both histological and molecular level and most of its biological mechanisms remain unclear. This fact, in combination with the high selectivity to drugs of blood brain barrier (BBB), makes challenging the searching for effective targeted therapies, that, till now, have failed. One of the most crucial aspects is that the tumour becomes symptomatic only when it is already of a high grade, making patient prognosis very poor, with a median survival from diagnosis of only about 15 months<sup>2</sup>.

According to the last World Health Organization guidelines (2021), GB is classified as an adulthood diffuse glioma with an isocitrate de-hydrogenase (IDH) wild type allelic profile. Differently, IDH-mutant gliomas are considered as less malignant astrocytomas. Histo-pathological diagnosis of GB is based on characterization of IDH genotype and/or presence of other tumoral items, like percentage of necrosis, microvascular proliferation, and EGFR amplification<sup>3</sup>.

Little less than 50% of GB patients with methylation in the promoter of O-6-methylguanine-DNA methyltransferase (MGMT), a DNA repair gene, show improved response to chemotherapy and better outcomes. Nowadays, detection of MGMT methylation in gliomas represents an established clinical routine, aimed at evaluating prognosis and managing treatment approach<sup>4</sup>.

Current standard treatment comprises surgical resection in combination with radiation therapy and temozolomide (TMZ) chemotherapy<sup>1</sup>. Moreover, administration of the corticoid agent dexamethasone (Dex) is necessary to counteract one of the most serious GB side effects, brain **oedema**, which is correlated with a worse prognosis.

As mentioned above, GB tissue appears highly heterogeneous, both at molecular and histological level<sup>5</sup>. One of the most important cell types, apart from differentiated tumoral astrocytes, are glioma stem cells (GSCs)<sup>6</sup>. GSCs have been determined in gliomas and play vital roles in driving tumour growth due to their competency in self-renewal and proliferation. Moreover, they are thought to be crucial at affecting treatment resistance<sup>7</sup>. They are typically localized within perivascular niches, and it is still unclear if they come from more differentiated GB cells that underwent de-differentiation programme or originate in the local brain stem cell pool<sup>8</sup>.

### **Blood brain barrier (BBB) impairment in GB**

BBB is a brain component highly compromised in GB and it is a crucial feature in the present study.

BBB is a highly organized and specialized structure of the central nervous system (CNS) essentially constituted by three main cellular components: i) endothelial cells, forming blood capillaries, ii) pericytes, inserted in vessel basal lamina, and iii) astrocyte end-feet. Like each barrier, BBB is designated to maintain tissue homeostasis<sup>8</sup>. Brain capillaries display a strictly regulated selectiveness on molecule flow, even during tumour progression, thus contributing to the poor chemotherapeutic efficacy<sup>2</sup>.

During tumour progression, vasculature becomes extremely heterogeneous and dysfunctional, being characterized by reduced tight junctions (TJs). Leaky and dysfunctional vessels of the compromised BBB allow blood liquids to flow into



the brain and induce pressure increase, thus promoting **oedema** development. In turn, pressure itself actuates as a barrier to chemotherapy, rendering oedema a booster of morbidity and mortality in GB patients<sup>5,9</sup>.

GSCs are a major responsible of tumour progression and of creation of the mentioned aberrant new vessels, aimed to sustain their metabolism. Neo-angiogenesis is observed both in the central areas of tumour, where the expanding and compressing mass is concomitant with the development of necrosis and associated with hypoxia-induced pathways, and in the peripheral ones. Interestingly, anti-angiogenic agents administered to counteract tumour growth, are effective only for an initial, short period, then tumour switches for genetic programmes that provide resistance both to hypoxia and drug delivery<sup>8,9</sup>.

Oedema in GB represents a serious side effect, associated with neurological symptoms, like headache, seizures, visual changes, walking and talking difficulties and even behavioural alterations<sup>10</sup>.

## **Zonulin**

Zonulin is a molecule involved in the regulation of tight junction (TJ) complex and it has been found in the endothelial wall of BBB. It was firstly described in 2000 as the endogenous analogue of *zonula occludens toxin* of the *Vibrio cholerae*, involved in the alteration of intestinal epithelial barrier<sup>11</sup>. TJs are complex structures, located at the edge of cell-to-cell contact, formed by transmembrane and cytoplasmic proteins and linked with the cytoskeleton. In epithelial and endothelial barriers, TJs accurately regulate permeability and absorption of molecules, under the modulation of physiological, pathological, and pharmacological stimuli<sup>12</sup>. Zonulin has reversible effects on TJs and communicates with innate and adaptive immune system to maintain barrier homeostasis<sup>10</sup>.

In 2008, zonulin was identified through proteome serum analysis as the **precursor** of haptoglobin (HP)-2, one of the two alleles of HP gene<sup>12</sup>. HP is produced in the liver and secreted into the bloodstream to bind free haemoglobin, thus preventing the formation of oxygen reactive species<sup>12</sup>. When zonulin undergoes post-translational cleavage, it is converted in HP and loses the ability both to bind its receptor and to increase epithelium permeability<sup>13</sup>.

### *Zonulin gene and signalling*

Zonulin gene is located at 16q22.2 chromosome (Gene ID: 3240). Two main alleles are described: HP-2 and HP-1<sup>12</sup>, being HP-2 the most frequent and correlated with a higher risk of developing inflammatory diseases<sup>13</sup>. Zonulin mRNA is firstly translated in a single polypeptide, then can undergo proteolytic cleavage in the endoplasmic reticulum to form HP protein<sup>12</sup>.

Zonulin transactivates EGFR via proteinase-activated receptor (PAR)-2, a G-protein coupled receptor<sup>14</sup>. Upon zonulin binding, phospholipase C hydrolyses phosphatidyl inositol, releasing second messengers and promoting TJs phosphorylation and actin polymerization<sup>15</sup>. This cascade causes the displacement and disassembling of junctional unit. Once zonulin signalling is over, TJs resume their baseline “closed” state<sup>16</sup> (**figure 1**).

Zonulin may represent a sort of indirect defence mechanism, addressed to eliminate exogenous antigens from paracellular compartment. For example, it was demonstrated that, in the intestine, both the gluten antigen *gliadin* and bacteria increase zonulin expression and secretion through C-X-C chemokine receptor (CXCR)-3 pathway<sup>14</sup>, resulting in the establishment of a pro-inflammatory cytokine milieu and mononuclear cell infiltration into the submucosa. The presence of inflammatory mediators, such as tumour necrosis factor- $\alpha$  and interferon- $\gamma$ , further increases permeability across the endothelial and epithelial layers. Furthermore, during the last decade, high blood levels of circulating zonulin became an established biomarker of intestinal permeability and were detected in obese patients in concomitance with hyperinsulinemia, hypertriglyceridemia, and elevated titres of inflammatory cytokines<sup>16</sup>.

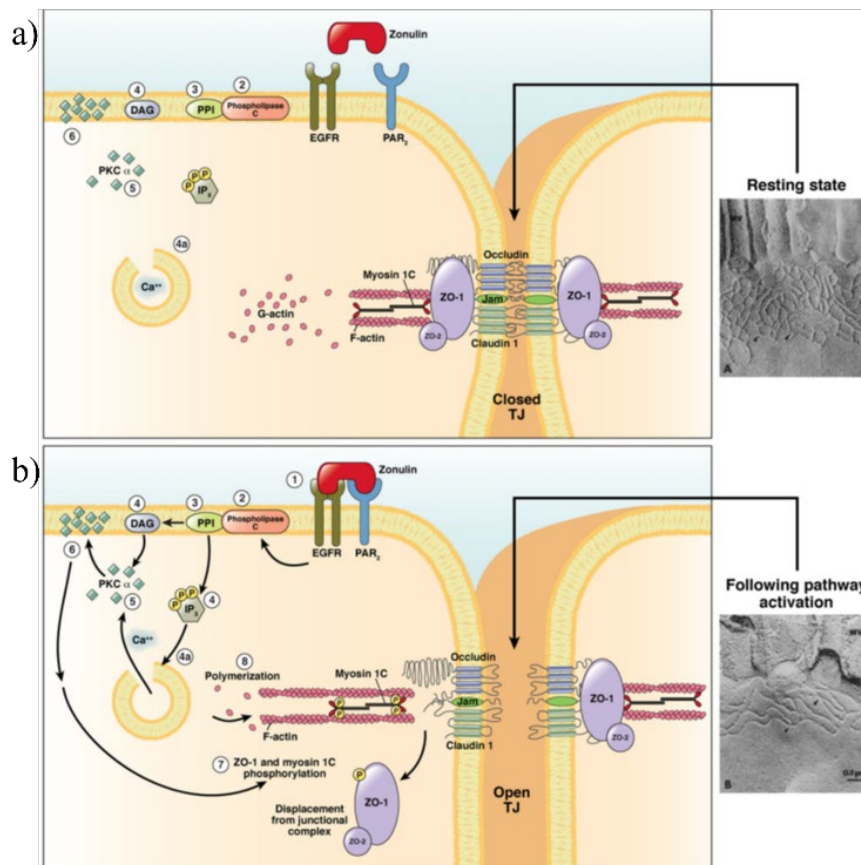


**Figure 1.** Representation of tight junction (TJ) disengagement upon zonulin receptor binding. a) Resting state: TJ proteins maintain their natural conformation, i.e., a “closed state”. b) Zonulin signalling leads to the activation of diacylglycerol-inositol triphosphate calcium pathway, which promotes actin polymerization and ultimately the loss of cell-cell contact (“open state”). In grey: electron microscopy photographs. EGFR: epidermal growth factor receptor. PAR-2: proteinase activated receptor-2. PPI: phosphatidyl inositol. IP-3: inositol 1,4,5-triphosphate. DAG: diacylglycerol. PKC- $\alpha$ : protein kinase C- $\alpha$ . ZO-1: zonula occludens-1. Image taken from *R. Lu et al.*<sup>16</sup>

## Zonulin in GB

Dysregulation of zonulin expression may contribute to disease states that involve altered barrier permeability and cell-to-cell contact, like celiac disease, colitis and even cancer. In GB, zonulin may be implied both in vasculature dysfunction and loss of intercellular contacts during tumour development. Although it is not clear which cell types and molecular mechanisms are involved in BBB damage in GB,

there is some evidence of zonulin expression in GB patients either at protein or RNA level.

Significant higher levels of zonulin in serum of GB patients were detected by proteomic analysis (MALDI-TOF mass spectrometry and Western Blot), compared to lower grade brain tumours<sup>17</sup>. In the same study, zonulin RNA was up-regulated ( $p < 0.0001$ ) in most GBs, compared to lower grade gliomas and healthy subjects.

In GB slides analysed by immunohistochemistry, zonulin immunoreactivity in interstitial and perivascular regions was correlated to the grade of the tumour<sup>17</sup>. Similarly, Skardelly et al.<sup>18</sup>, using immunofluorescence technique, showed that in the highest-grade GBs, BBB disruption was a relevant feature, revealed by co-localization of zonulin and GSI-agglutinin, a marker of vessel damage<sup>18</sup>.

*In vitro*, zonulin in the medium promoted mobilization of a human neural glioma stem cell line across a rat BBB model. Zonulin levels were correlated to barrier degradation and loss of resistance and to a higher migration capacity of stem cells towards tumour site<sup>19</sup>. However, further studies should be performed using a more reliable humanized model and better techniques to measure permeability<sup>20</sup>.

Finally, Sanchez et al. discovered that only zonulin mRNA was overexpressed in a glioma cell line, U-87MG, differently from hepatoma cell lines HepG2, where elevated levels of zonulin were present either as a transcript and a protein. This suggests that zonulin mRNA expression may require further investigation<sup>21</sup>.

## HYPOTHESIS AND AIMS OF THE STUDY

Zonulin is a molecule implied in barrier permeability impairment and it is overexpressed in serum of high-grade glioma patients<sup>18</sup>.

Therefore, the first hypothesis was that zonulin was expressed in GB and may have a role in dysregulation of BBB disruption and subsequent establishment of oedema<sup>5,9</sup>. In this regard, we supposed that zonulin levels were associated with oedema volume.

In addition, was hypothesized that levels of zonulin might be related to prognosis, basing on the described correlation between higher levels of zonulin and more malignant GB forms<sup>17,18</sup>.

Was also supposed that zonulin was more expressed in GB samples than in glioma cell lines U-87MG and U-118MG, since zonulin is a molecule inducible by microenvironmental factors<sup>16</sup>, as those of the *in vivo* context.

Finally, was proposed that zonulin may be more expressed in GSCs compared to glioma cell lines. In fact, these cells promote the formation of new dysfunctional vasculature, characterized by a high degree of TJs disengagement<sup>5,9</sup> and elevated levels of zonulin<sup>14</sup>.

Since there is some evidence of zonulin implication in high-grade gliomas, but some aspects remain unclear, the main aim of the present study was to clarify the role of zonulin in GB biology.

To experimentally assess this purpose, the following specific aims were established:

1. To measure zonulin and HP serum levels in GB patients.
2. To assess zonulin RNA and protein expression in GB samples, in glioma cell lines U-87MG and U-118MG, and in GSCs obtained from de-differentiation of U-87MG cells *in vitro*.

3. To investigate correlations between zonulin (and HP) values in serum and survival outcomes.
4. To investigate correlations between zonulin levels in tumour samples and clinical parameters/survival outcomes.
5. To compare zonulin expression among patients, glioma cell lines U-87MG and U-118MG, and GSCs.

## MATERIALS AND METHODS

### **GB patients**

A total of 21 patients were included in the study, after a diagnosis of GB-IDH wild type.

Clinical variables analysed in the study were acquired from individual medical history and comprised:

- Karnofsky index, a functional parameter which, if <70, indicates patient inability to carry out daily activities or active work.
- Peritumoral oedema, tumoral contrast-enhancement and tumoral necrosis volume, i.e., parameters evaluated in presurgical magnetic resonance imaging (MRI).

Molecular data were obtained from anatomopathological report:

- Ki67: an established marker of proliferating cells.
- MGMT methylation: a molecular predictor for treatment election<sup>4</sup>.

Radiological analysis was performed using *Oncohabitats* platform (<https://www.oncohabitats.upv.es/>), an online tool that allows to segment images from the presurgical MRI, providing the peritumoral oedema, the tumoral contrast-enhancement and the tumoral necrosis volume.

### **Tissue collection**

Tumour samples were collected after surgical resection at *Hospital Universitario de Canarias* (Tenerife, Spain). Informed consent was previously acquired, and anonymous identification guaranteed, according to ethics committee guidelines (project code: CHUC\_2019\_59). Samples coming from tumour recurrences were excluded.

In addition, a blood sample was obtained from 14 of the 21 patients included in the study.

### **Cell lines and cell culture**

Two human glioma cell lines were used for the study: U-87MG, representing a GB grade III-IV and U-118MG, corresponding to a GB grade IV, both purchased from ATCC (Cat #HTB-14 and Cat #HTB-15, respectively). Cell lines were seeded in T75 flasks at a seeding density of approximately 1,000,000 cells, in standard medium (SM). SM was prepared as follows: Dulbecco's modified Eagle's medium/Ham's F-12 (DMEM/F12, Cat #11330032), containing L-Glutamine and 15mM HEPES, supplemented with 10% foetal bovine serum (FBS, Cat #S1810) and antibiotics (59 mg/L Penicillin, Cat #P3032; 100 mg/L Streptomycin; Cat #S9137; 25 mg/L Amphotericin, Cat #A2411). Cells grew in monolayer in incubator at 5% CO<sub>2</sub> at 37°C, and medium was refreshed every two days. Upon reaching confluence, cells were treated with trypsin-EDTA (Cat #L0930) to induce dissociation among them and from plate surface. Then, cells were counted with the automatic cell counter TC20 (BIORAD) using Cell Counting Kit (Cat #1450003). Finally, cell pellets were collected in aliquots of approximately 200,000 alive cells and stored at -20°C for next experimental use. For each cell line, a total of 20 aliquots were stored: 10 destined to RNA extraction and complementary DNA (cDNA) synthesis, and 10 for protein lysates.

### **Neurosphere induction from U-87MG cell line**

U-87MG parental cell line was seeded at the concentration of approximately 100,000 cells/ml in neural stem cell medium (NSCM). NSCM was prepared based on the recipes published by Iacopino et al.<sup>22</sup> and Yu et al.<sup>23</sup>, as follows: DMEM/F12, containing L-Glutamine and 15mM HEPES (Cat #11330032), supplemented with antibiotics (59 mg/L Penicillin, Cat #P3032; 100 mg/L



Streptomycin; Cat #S9137; 25 mg/L Amphotericin, Cat #A2411), recombinant human epidermal growth factor (rhEGF, Cat #236-EG-200) 20 ng/ml, basic fibroblast growth factor (bFGF, Cat # 233-FB-025/CF) 20 ng/ml and B-27 additive 1X (Cat #A3353501).

To obtain neurospheres, multiple growing conditions were established, i.e., cells were seeded in either no-adherent adherent and plates, both in SM and NSCM, basing on information available in literature<sup>22,23,24</sup>:

- Adherent plates (6-well plates): U-87MG cells were seeded at a density of 100,000 cells/well with SM, that was replaced with NSCM following two different protocols: 1/3 of medium was replaced every 24 hours (i.e., “progressive” replacement) or the whole medium was replaced every 48 hours (i.e., “total” replacement). In both conditions a control well was included. All experiments conditions were carried out in duplicate. Neurosphere formation was daily monitored, and pictures of the same field were taken at 10X magnification using OLYMPUS CKX53 microscope, with DP23 digital camera and the associated imaging software cellSens 4.1. Pellets (n=12) were all collected after 96 hours.
- No-adherent plates (35 mm): 100,000 cells were seeded either with SM or NSCM. Experimental conditions were carried out in duplicate. Neurosphere formation was daily monitored, and pictures of the same field taken at 10X magnification using OLYMPUS CKX53 microscope, with DP23 digital camera and the associated imaging software cellSens 4.1. Pellets (n=4) were all collected after 72 hours.

### **RNA extraction and cDNA synthesis**

GB samples, upon surgical resection were maintained in TRIzol Reagent (Invitrogen, Cat #15596026) to optimally preserve their original characteristics

and reach bigger RNA yield. Then, they were mechanically grinded and lysed using a handheld Dounce homogenizer. Subsequently, the whole RNA was extracted using Aurum Total RNA Mini Kit (BIORAD, Cat #7326820), according to manufacturer's instructions. After RNA quantification with Nanodrop, cDNA was synthesised using iScript cDNA Synthesis Kit (BIORAD, Cat #1708890) and synthesis reaction took place in DNA thermal cycler PERKIN ELMER, as follows: priming at 25°C for 5 minutes, reverse transcription (RT) at 46°C for 20 minutes and RT inactivation at 95°C for 1 minute (additional optional holding at 4°C).

From cell pellets, the whole RNA was extracted, using Aurum Total RNA Mini Kit (BIORAD, Cat #7326820), according to manufacturer's instructions. The cDNA was reversely transcribed from total RNA using iScript cDNA Synthesis Kit (BIORAD, Cat #1708890), following the same protocol as for GB samples.

### **Quantitative real-time polymerase chain reaction (qRT-PCR)**

Starting sample was the whole cDNA, obtained following the protocol explained above.

To address amplification only towards zonulin cDNA sequence, specific oligonucleotides were designed using OMIGA server, with the reference transcript sequence found in NCBI Gene database (ref. NM\_005143.5). Then, sequence specificity was checked using BLAST online tool. The detailed primer sequences for zonulin are as follows:

Forward (F): 5'-TCTACACCCTAACTACTCC-3'

Reverse (R): 5'-CCTACTTCTGCATAATCC-3'

Primer pair (F+R) dilution was prepared at 1.6 µM and loaded with cDNA and SsoFast EvaGreen Supermix (BIORAD, Cat #1725200), composed of dNTPs, Sso7d-fusion polymerase, MgCl<sub>2</sub>, EvaGreen dye and stabilizers. EvaGreen dye increases its fluorescence upon intercalation with double-strand-DNA, so its

registered signal is proportional to the amount of the accumulated product, resulting from amplification of starting target cDNA.

The equipment used for qRT-PCR was C1000 thermal cycler (BIORAD), with the associated software CFX96 (BIORAD). Primer efficiency and annealing temperature gradient were tested to optimize qRT-PCR conditions. Then, the reaction was performed, using the following protocol: i) 1 cycle of enzyme activation at 95°C for 30 seconds; ii) 44 cycles of denaturation at 95°C for 5 seconds and annealing-extension at 55°C for 5 seconds; iii) 1 cycle of melt curve at 65°C for 5 seconds. This last step is particularly useful to check any possible nonspecific dye binding. Each sample was loaded in triplicate at a final volume of 10µl/microwell. Amplification data were analysed using CFX96 software.

To assess the changes in zonulin RNA expression, its threshold amplification cycle (Ct) was compared to that of a reference gene, i.e., the housekeeper gene beta-actin, using the “ $2^{\Delta C_t}$  method”<sup>25</sup>. It represents a convenient way to obtain a relative quantification of a gene of interest. The detailed primer sequences for beta-actin are as follows:

F: 5'-CTTCCTTCCTGGGCATGG-3'

R: 5'-GCCGCCAGACAGCACTGT-3'

## **Western Blot**

Cell pellets and frozen fragmented tissues were directly resuspended in Laemmli sample buffer (LSB) 1X and stored at -20°C until its use for Western Blot (WB) assay. LSB contains: i) denaturalizing and reducing agents, to linearize proteins and allow their unidirectional running during electrophoresis; ii) a dye tracker, to visualize protein separation during electrophoresis; iii) detergents, to lysate cell membranes and release protein content.

Protein samples were not quantified because the final analysis would be based on the relative measurement of protein amount, i.e., compared to the total protein quantity transferred from the gel to the membrane.

Polyclonal rabbit anti-human zonulin antibody (Abxexa, Cat #abx109849) was used for WB assay, at the dilution of 1:500. Protein extracts from mouse stomach and liver samples were first loaded as positive controls for anti-zonulin, in accordance to manufacturer's instructions. In addition, monoclonal mouse anti-human CD133 (Invitrogen, Cat #MA1-219), previously tested in the laboratory, was employed, at the dilution of 1:1,000, to verify stemness in neurospheres<sup>26</sup>.

Gel was prepared with a percentage of acrylamide such as permitting an optimal resolution of the protein of interest, i.e., depending on its molecular weight (MW). Since zonulin MW is around 50 kDa, gel was prepared at 12% acrylamide. Differently, for CD133 detection, an 8% acrylamide gel was used, being CD133 expected MW around 130 kDa.

Both tissue samples and cell pellets, previously resuspended in LSB 1X, were submitted to denaturalizing temperature (95°C) for 10 minutes. This step would improve protein separation during gel electrophoresis. Samples were loaded in a final volume of 15 µl/well. A MW marker was also loaded. Running phase took place in the appropriate buffer at room temperature and lasted around 1 hour at 100-150 V.

Then, proteins were transferred from the gel to a poly-vinylidene-fluoride membrane (Millipore, Cat #IPVH00010), in the appropriate buffer at 100 V, during 1 hour at 4°C. Sandwich was carefully assembled, focusing on respecting sample loading order, removing bubbles, and positioning the blot on the cathode side. Subsequently, membrane was blocked in a 5% non-fat dry milk diluted in phosphate-buffered-saline (PBS) 1X-0.1% Tween 20 (PBS-T), to prevent unspecific antibody binding. Total protein transference was checked by gel staining with Coomassie Blue (CB). Membrane was incubated with the primary antibody over/night (O/N) at room temperature.

The day after, membrane was washed for 10 minutes, 3 times in PBS-T 1X, then incubated with the secondary antibody for 1 hour at room temperature. Secondary antibodies were conjugated to horseradish peroxidase (HRP), an enzyme able to generate a recordable signal when a chemiluminescent substrate is added. An HRP-conjugated anti-rabbit at 1:50,000 (Cat #F9887) and an HRP-conjugated anti-mouse at 1:5,000 (Cat #A5906) were used. Finally, membrane was washed for 10 minutes, 3 times in PBS-T 1X and the chemiluminescent substrate applied, according to the manufacturer's recommendations (Immobilon, Millipore, Cat #WBKLS0100).

Images were collected using ChemiDoc equipment (BIORAD) and analysed by Image Lab 6.1 software (BIORAD). First, target protein MW was checked using the colorimetric image as a reference. Then, bands were quantified with respect to the total amount of proteins transferred to the membrane, using the CB image as a reference.

### **Immunofluorescence (IF)**

U-87MG and U-118MG cells were seeded in 4-well plates, coated with 15mm coverslips, using SM for 24 hours. Coverslips were previously treated with a combination of poly-L-lysine and gelatine to improve cell adherence. However, this condition limits cell growth and wellness: so, cells were seeded close to confluence density (around 50,000 cells/cm<sup>2</sup>).

After 24 hours of culture, cells were fixed: medium was carefully removed, cells were washed with PBS 1X for 3 times and methanol 100% was added to each well. Plates were incubated for 6 minutes at -20°. At this point, sterility conditions were quit. Upon a further washing round, fixed cells were stored at 4°C O/N, in a minimum volume of PBS 1X to prevent dehydration.

Then, blocking phase was realized, incubating cells in universal blocking solution (UBS) during 30 minutes in agitation. UBS was prepared with 1% bovine serum

albumin (BSA), 0.1% gelatine, 0.5% Triton X-100 (permeabilizing factor), 0.05% azide (to prevent contamination), diluted in an appropriate PBS 1X at pH 7.2-7.4. ICC-specific PBS 10X stock (100 ml) is made of 1.9 g Na<sub>2</sub>HPO<sub>4</sub>, 0.32 g NaH<sub>2</sub>PO<sub>4</sub>, 9 g NaCl.

Subsequently, UBS was removed and primary antibody rabbit anti-human zonulin (Abxexa, Cat #abx109849), was added at a dilution of 1:500, in UBS, for 1 hour at room temperature in agitation. A negative control was included, meaning that a volume of UBS was added instead of primary antibody.

Upon washing for 10 minutes, 3 times, with tris-buffer-saline-0.05% Tween-20 (TBS-T) 1X, pH 8.4, a fluorescent secondary antibody (anti-rabbit IgG-FITC, Cat #F9887) was added at a concentration of 1:200 (diluted in TBS-T 1X) and incubated in darkness during 1 hour at room temperature in agitation. From here on, next steps were all performed respecting darkness conditions, not to damage fluorescence signal.

To remove the excess of secondary antibody, cells were washed with TBS-T 1X for 10 minutes, for 3 times. Then, coverslips were carefully mounted on glass slides with a drop of ProLong®Diamond Anti-fade Mountant (Invitrogen, Cat #P36961), a glycerol-based mounting medium containing the DNA marker DAPI. Slides were then stored in dark at +4°C until imaging acquisition.

Immunostaining was analysed with fluorescence microscope OLYMPUS BX50 and the associated software DP-BSW.

### **Enzyme-linked immunosorbent assay (ELISA)**

Human Zonulin ELISA Kit (Elabscience, Cat #E-EL-H5560) and Human HP(Haptoglobin) ELISA Kit (Elabscience, Cat #E-EL-H6078) were employed to measure serum levels of zonulin and HP.

ELISA microplate was prepared by covering each microwell with zonulin (or HP) specific antibody. Then, serum samples were loaded, and antigens immobilized to

the support thanks to the presence of the specific antibody. Subsequently, a detection biotinylated antibody, specific for zonulin (or haptoglobin), was added, thus allowing the formation of the so-called “sandwich” (the antigen is trapped between two specific antibodies: one immobilized to the support and one in solution).

Upon incubation with the detection antibody and the removal of unbound material through washing, an HRP-conjugated secondary antibody was added. Finally, a further washing step was performed and the substrate for the enzymatic reaction added.

Only wells containing human zonulin (or haptoglobin) appeared coloured in blue: to finalize the enzyme-substrate reaction, a stop solution was added, thus making the dye turning into yellow. At this point, colour intensity was measurable as optical density (OD) using a spectrophotometer, at a wavelength of  $450 \text{ nm} \pm 2 \text{ nm}$ . OD was proportional to the concentration of the target molecule.

Standard calibration curve for each ELISA microplate was realized in duplicate. Intra and inter assay variation coefficients were accepted if below 10%.

### **Image analysis**

All pictures taken during microscopy analysis were saved in “.jpg” format, to allow exportation and examination using other programmes. ImageJ 1.54d software was used to merge immunofluorescence images and to measure neurosphere diameters.

### **Statistical analysis**

Data analysis was carried out using Excel spreadsheet from Microsoft Office 365 and the statistics software Jamovi 2.2.5.

To assess if data followed a normal distribution, Shapiro-Wilk test and Kolmogorov-Smirnov test were performed. These two tests assume as a null

hypothesis that data follow a normal distribution, so if p-value is below statistical significance, the assumption of a normal distribution will be rejected, and non-parametric tests must be employed to analyse data.

Statistical significance was established in  $p < 0.05$ .

The examined populations resulted not to be normally distributed. Moreover, sample sizes were reduced (GB samples:  $n=21$ ; serum samples:  $n=14$ ; glioma cell lines:  $n=10$ ; neurospheres:  $n=6$ ). For these reasons, non-parametric tests were employed for statistical analysis.

To compare continuous variables among groups, non-parametric Kruskal-Wallis test was employed.

For correlation analysis with clinical and molecular data, Fisher's Exact test and Chi-Square test were used for categorical variables, whilst Mann-Whitney U. test was performed for continuous values.

In addition, a survival analysis was carried out for progression-free survival (PFS), using the Log-Rank test.



## RESULTS

### **Analysis of zonulin and haptoglobin expression in patient serum**

Zonulin and haptoglobin serum values were dichotomized, using the medians as a cutoff (zonulin  $p50=44.5$ ; haptoglobin  $p50=198.85$ ). Survival analysis revealed that patients with “high” levels of zonulin presented a worse prognosis than those with “low” levels (103 vs 252 days; Log-Rank test:  $p=0.012$ ) (**figure 2**). Conversely, patients with “high” levels of haptoglobin presented better prognosis than those with “low” levels (102 vs 252 days; Log-Rank test:  $p=0.038$ ) (**figure 3**). No significant correlation existed between zonulin and haptoglobin serum levels (Spearman correlation coefficient= $-0.020$ ;  $p=0.946$ ), neither between zonulin levels in serum vs tumour samples (WB data) (Spearman correlation coefficient= $-0.011$ ;  $p=0.970$ ).

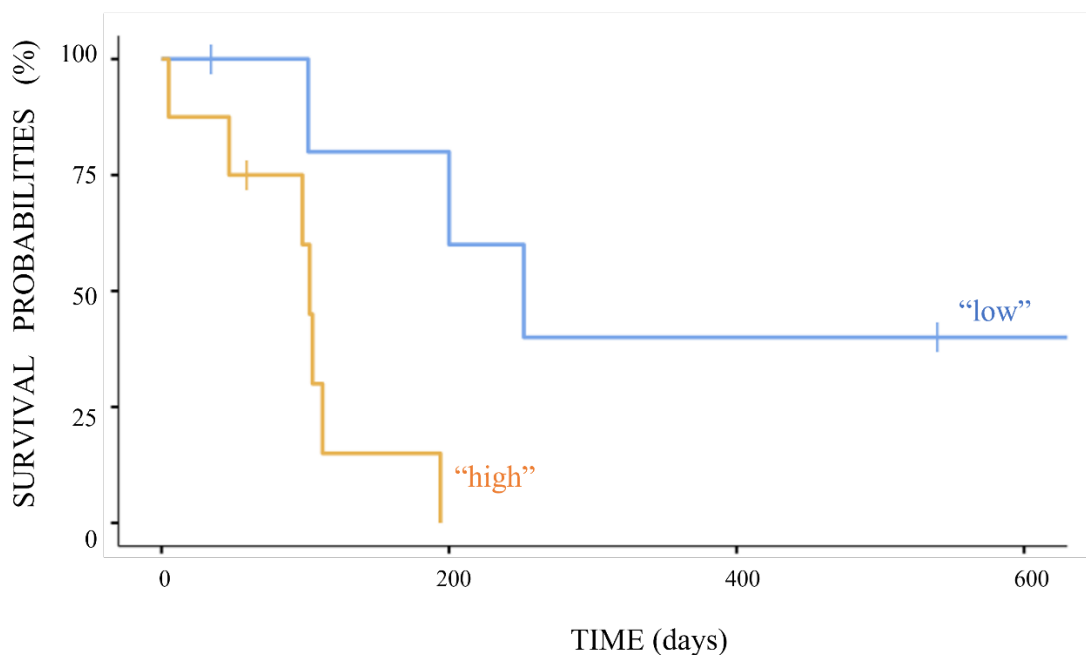


**Figure 2.** Survival plot related to zonulin serum levels. “High” or “low” zonulin expression in serum is correlated to a worse or better progression-free survival (days), respectively (Log Rank:  $p=0.012$ ). †: censored data.

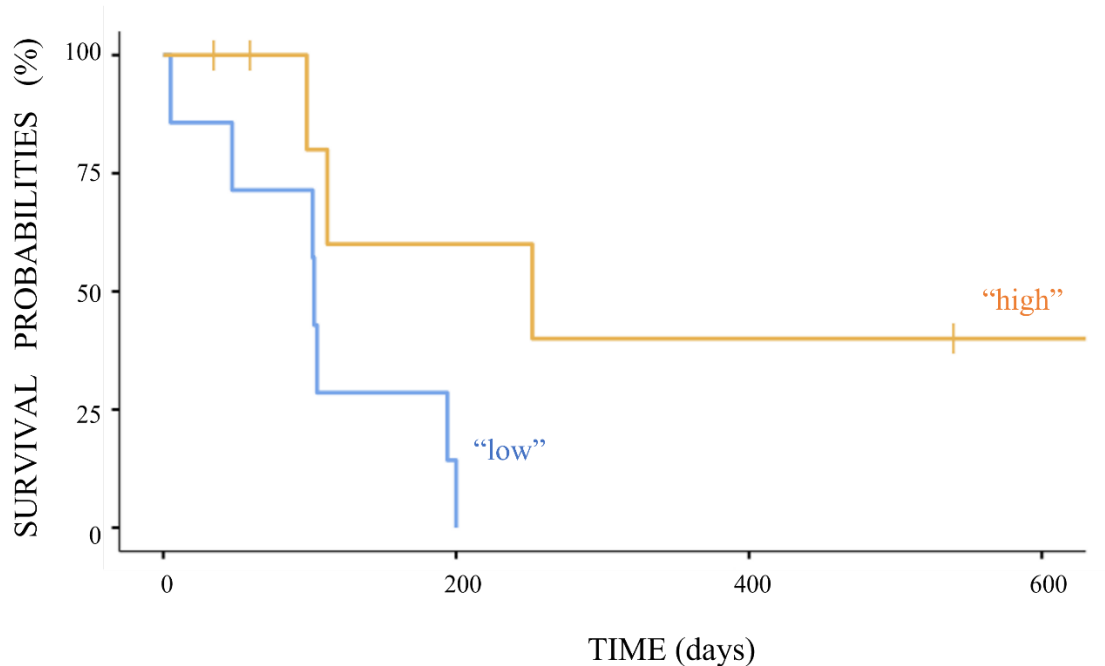


**Figure 3.** Survival plot related to HP serum levels. “High” or “low” HP expression in serum is correlated to a better or worse progression-free survival (days), respectively (Log Rank:  $p=0.038$ ). †: censored data.

### **Analysis of zonulin expression in patient tumour samples**

Clinical, radiological, and molecular features of the 21 patients included in zonulin expression analysis are resumed in **table 1**. Karnofsky index, contrast enhancement, type of resection and MGMT methylation are reported as absolute numbers (out of 21) and corresponding frequencies (%). Age, contrast enhancement volume, oedema volume, necrosis volume, Ki67, zonulin RNA and protein values are expressed as means (and corresponding standard deviations).

<b>Table 1. Clinical, radiological, and molecular features of patients included in the analysis of zonulin expression in tumoral samples</b>		
Age		65.33 (SD=11.87)
Gender (male:female)		10:11
Karnofsky<70		2 (9.5%)
Contrast enhancement	Periferic	8 (38.1%)
	Heterogeneous	13 (61.9%)
Contrast enhancement volume (cc)		19.76 (SD=14.19)
Oedema volume (cc)		59.24 (SD=36.6)
Necrosis volume (cc)		8.46 (SD=9.48)
Resection	Partial	2 (9.5%)
	Subtotal	4 (19.0%)
	Total	15 (71.4%)
Ki67 (%)		27.4 (SD=19.53)
MGMT methylation		10 (47.6%)
Zonulin (mRNA)		950.2 (SD=780.03)
Zonulin (Protein)		1245.23 (SD=1670.56)
SD: standard deviation; cc: cubic centimeters.		

As expected, zonulin RNA expression was detected in GB samples (mean value: 950.2±780.03).

At protein level, zonulin expression was quantified by WB. Zonulin antibody was checked in positive controls (**figure 4**).

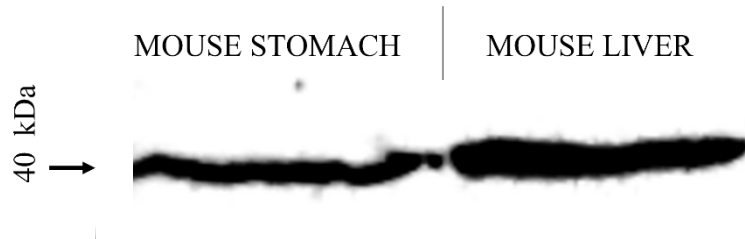


**Figure 4.** Zonulin antibody test in positive controls. Protein extracts from mouse stomach and liver were used to check rabbit anti-human zonulin functionality, according to manufacturer's instructions. Zonulin MW is lower in mouse than in human (MW  $\approx$  40 kDa). Dilution: 1:500.

In some cases, double bands around the expected MW of 50 kDa were observed (**figure 5**). In this regard, all the signal detected around the level of interest was included.

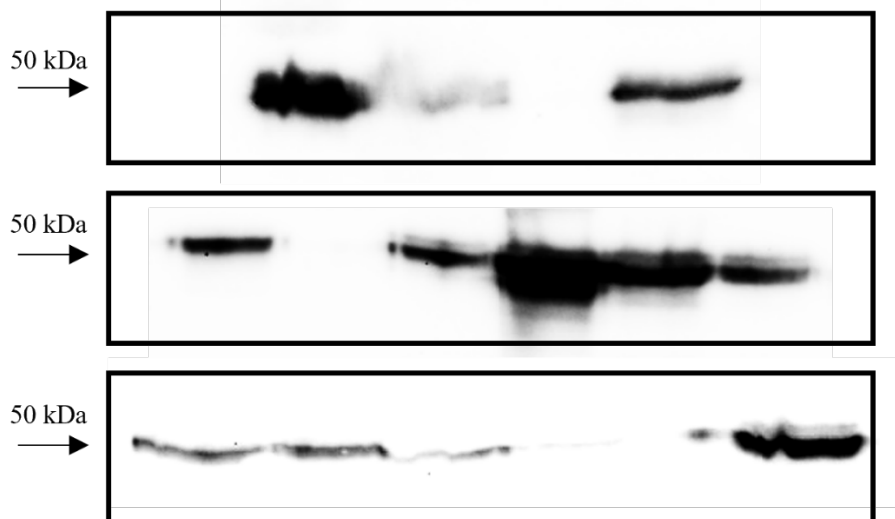


**Figure 5.** Examples of WB acquisitions for GB tumoral probes. Zonulin band corresponds to a MW of approximately 50 kDa.

Zonulin expression values obtained by WB were dichotomized, using as a cut-off the median ( $p_{50}=406.79$ ). Comparison between “low expression” and “high expression” groups is shown in **table 2**. Karnofsky index, contrast enhancement, type of resection and MGMT methylation are reported as absolute numbers and corresponding frequencies (%). Age, contrast enhancement volume, oedema volume, necrosis volume, Ki67, zonulin RNA and protein values are expressed as means (and corresponding standard deviations).

<b>Table 2. Comparison between groups of “high” vs “low” zonulin expression in tumoral probes</b>				
<b>Variable</b>		<b>Low zonulin (n=11)</b>	<b>High zonulin (n=10)</b>	<b>p-value</b>
Age (years)		61.55 (SD=14.00)	69.5 (SD=7.66)	0.341 <sup>a</sup>
Gender (male:female)		4:7	6:4	0.395 <sup>b</sup>
Karnofsky<70		2 (18.2%)	-	0.476 <sup>b</sup>
Contrast enhancement	Periferic	6 (54.5%)	2 (20.0%)	0.183 <sup>b</sup>
	Heterogeneous	5 (45.5%)	8 (80.0%)	
Contrast enhancement volume (cc)		12.91 (SD=10.31)	28.13 (SD=14.20)	<b>0.020<sup>a</sup></b>
Oedema volume (cc)		42.44 (SD=19.14)	79.78 (SD=43.13)	<b>0.037<sup>a</sup></b>
Necrosis volume (cc)		6.50 (SD=9.81)	10.85 (SD=9.01)	0.152 <sup>a</sup>
Resection	Partial	1 (9.1%)	1 (10.0%)	0.990 <sup>c</sup>
	Subtotal	2 (18.2%)	2 (20.0%)	
	Total	8 (72.7%)	7 (70.0%)	
Ki67 (%)		26.2 (SD=17.62)	28.6 (SD=22.17)	0.880 <sup>a</sup>
MGMT methylation		6 (54.5%)	4 (40.0%)	0.670 <sup>b</sup>
Zonulin (mRNA)		865.9 (SD=932.96)	1026.06 (SD=655.51)	0.567 <sup>a</sup>
PFS (days)		194 [57.6 – 330.3]	98 [34.0 – 162.0]	0.079 <sup>d</sup>
SD: standard deviation; cc: cubic centimeters.				

<sup>a</sup> Mann-Whitney U.

<sup>b</sup> Fisher's Exact test.

<sup>c</sup> Chi-Square.

<sup>d</sup> Log-Rank test.

Patients with “high” zonulin expression had also an increased contrast enhancement volume (28.13 vs 12.91 cc;  $p=0.020$ ) (**figure 6**) and oedema volume (79.78 vs 42.44 cc;  $p=0.037$ ) (**figure 7**) in pre-surgical MRI. In addition, patients with elevated zonulin expression showed a more heterogeneous contrast enhancement (80.0% vs 45.5%), although this difference did not reach statistical significance.

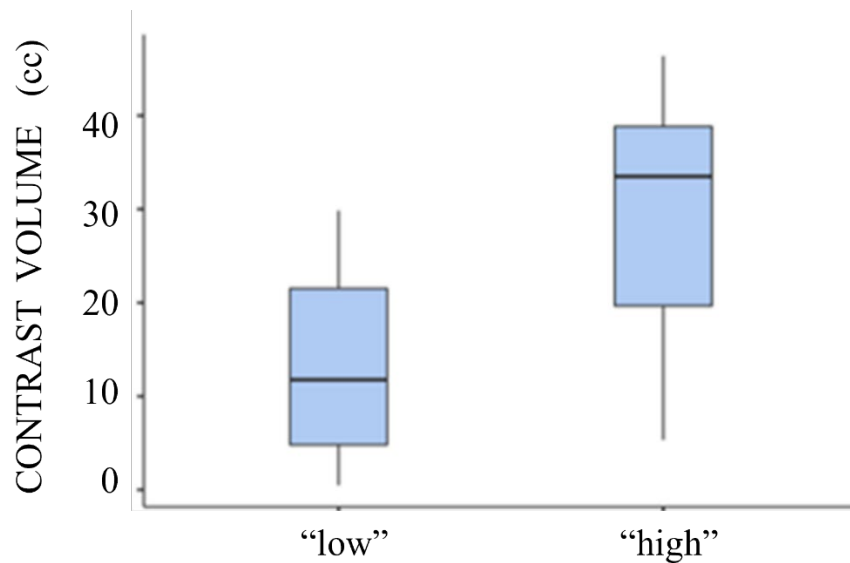


**Figure 6.** Box plot representing correlation between contrast volume (cc) and zonulin expression in tumour samples. Higher levels of zonulin are associated to higher contrast volume ( $p=0.020$ ). “low”:  $n=11$ . “high”:  $n=10$ .

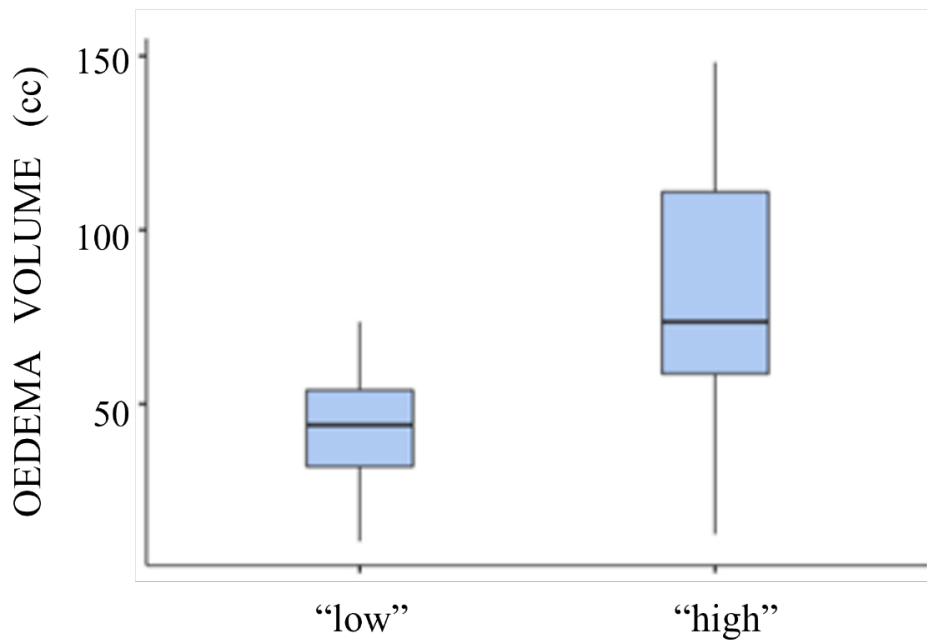


**Figure 7.** Box plot representing correlation between oedema volume (cc) and zonulin expression in tumour samples. Higher levels of zonulin are associated to higher oedema volume ( $p=0.037$ ). “low”:  $n=11$ . “high”:  $n=10$ .

The rest of the clinical and molecular variables did not exhibit any difference between the two groups. Nevertheless, it is worthy to highlight the existence of a positive trend in favour of a low expression of zonulin with respect to the prognosis, i.e., progression-free survival (PFS). In this sense, patients with low levels of zonulin presented a major PFS than patients with high expression of zonulin (194 vs 98 days;  $p=0.079$ ) (**figure 8**).

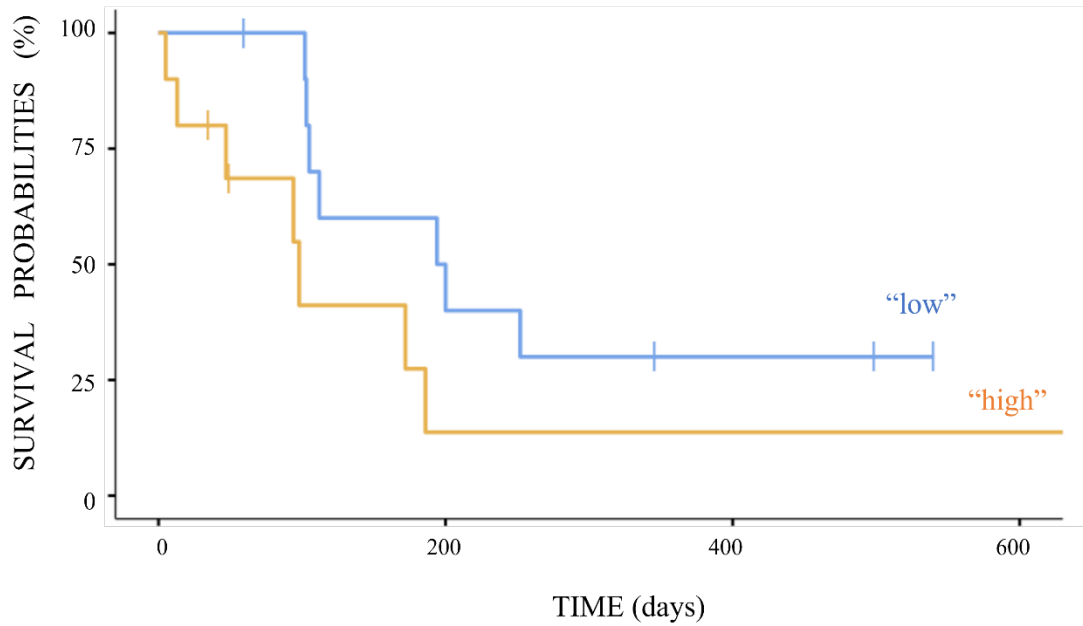


**Figure 8.** Survival plot related to zonulin expression in GB samples. “High” or “low” zonulin expression in tumour sample is correlated to a worse or better progression-free survival (days), respectively, although this difference is not significant (Log Rank:  $p=0.079$ ). †: censored data.

### Analysis of zonulin expression in U-87MG and U-118MG cell lines

Zonulin RNA was expressed in glioma cell lines (U-87MG mean value:  $507.88 \pm 721.50$ ; U-118MG mean value:  $939.71 \pm 1183.70$ ) and no significant difference was detected between groups.

Zonulin protein was also expressed (U-87MG mean value:  $7.48 \pm 6.82$ ; U-118MG mean value:  $44.60 \pm 67.68$ ) without significant difference between the two groups.

In **figure 9**, pictures of zonulin immunostaining in U-87MG and U-118MG cells are reported (40X magnification). Zonulin immunoreactivity was detected in nuclei.



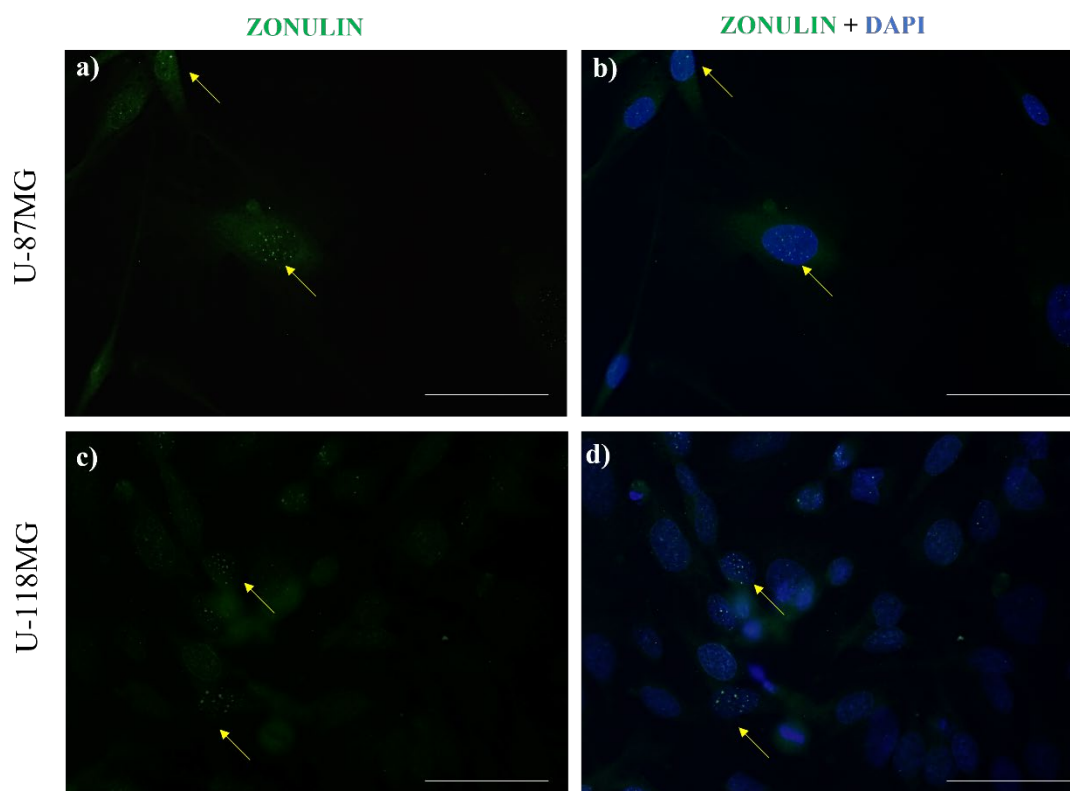


**Figure 9.** Immunolabeling of zonulin in U-87MG (a,b) and U-118MG (c,d) cell lines. Cells were stained with rabbit anti-zonulin antibody 1:500. a,c) green channel (zonulin). b,d) merge of the green (zonulin) and the blue (DAPI) channel, the latter evidencing DNA. Yellow arrows indicate zonulin location in nuclei. Pictures were taken at 40X magnification. Scale bar: 100  $\mu$ m.

### **Analysis of neurosphere development and characterization**

Neurosphere development from U-87MG cell line was daily monitored and photographed.

In no-adherent plates, U-87MG cells started growing in suspension (i.e., as spheres) after 24 hours, in both standard medium (SM) and neural stem cell medium (NSCM), probably due to the lack of adhesive support. So, neurosphere

phenotype appeared similar in the two mediums. Therefore, we investigated possible differences in growth rate, by comparing sphere diameters at 24, 48 and 72 hours between SM and NSCM conditions. At 72 hours, spheres grown in NSCM were bigger than those grown in SM, although no statistical significance was reached (means: 74.80  $\mu\text{m}$  vs 66.20  $\mu\text{m}$ ) Conversely, overall size increment was major for spheres grown in SM than NSCM (at 72 hours: 203.10% vs 125.94%, ns). Statistical significance was detected in daily size increment, but only within each group (**figure 10**).

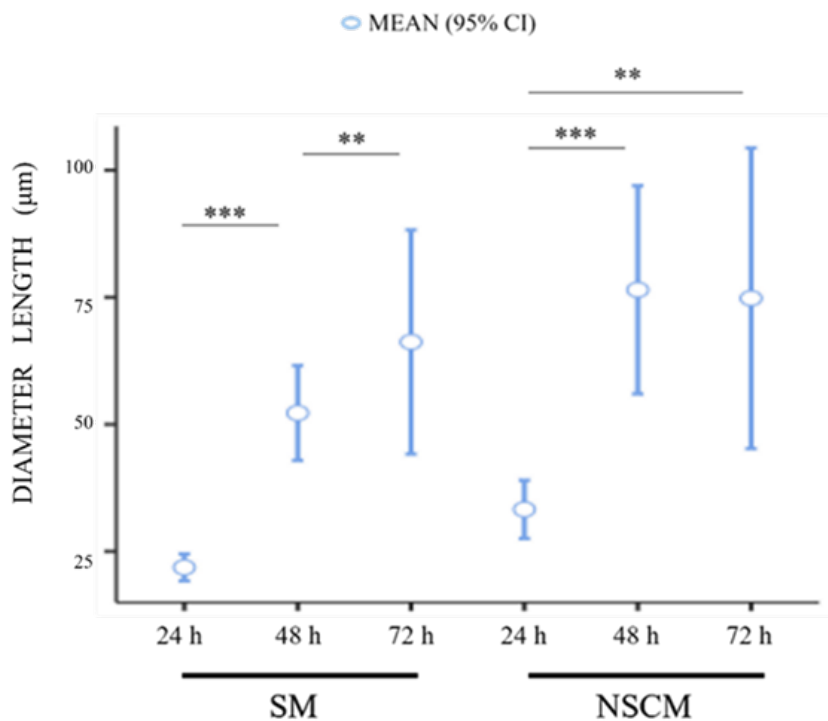


**Figure 10.** Neurosphere diameters in no-adherent plates. Descriptive plot of diameters, relatively to neurospheres cultured in no-adherent plates, either in standard medium (SM) or neural stem cell medium (NSCM). Measurements were realized at 24, 48 and 72 hours. No-parametric Kruskal-Wallis test was performed. \*\*:  $p < 0.005$ . \*\*\*:  $p < 0.001$ . For each condition were realized 15 measurements.

In adherent plates, U-87MG cells started growing, as expected, in a monolayer, since they were initially seeded in SM. Along with NSCM addition, cells lost their native shape and surface adherence, and began to float as spheres. Some qualitative differences were observed if replacement of medium were performed all at once (“total”) or in a “progressive” way: i) in “total” replacement condition sphere development was quicker than in the “progressive” one, and less debris were found in the medium; ii) in “total” replacement condition a higher number of cells had converted into spheres at the end of the experiment (96 hours).

To verify neurosphere identity as GSCs, WB assay for CD133 stemness marker was performed. CD133 resulted expressed in these cells, providing confirmation on their GSC profile. However, CD133 was also expressed by normal U-87MG cells. A qualitative increase in CD133 expression was observed in spheres that undergone a progressive addition of NSCM, compared to other groups (**figure 11**) (no statistical test was performed, group size: n=2).

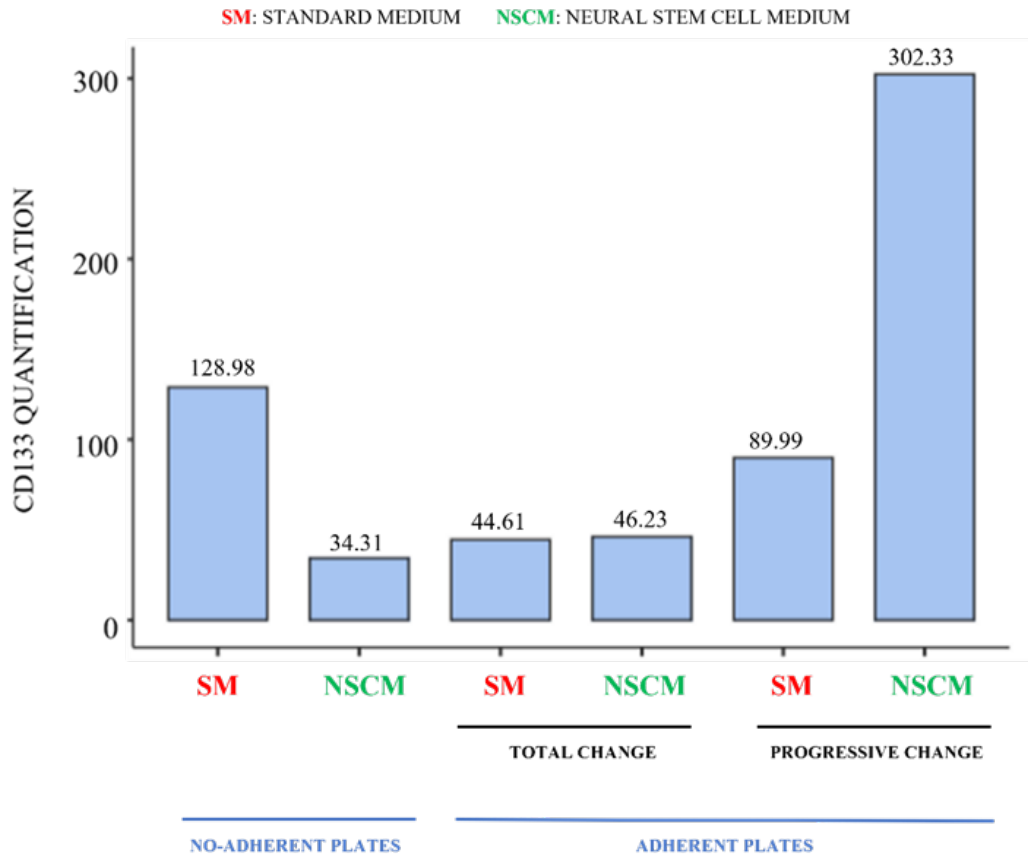


**Figure 11.** CD133 expression in neurospheres. Histogram representing CD133 relative quantification (WB) of neurospheres, cultured in no-adherent or adherent plates, either in standard medium (SM) or neural stem cell medium (NSCM). For adherent plates, a total or progressive change of medium was performed. Quantification data reported in the graph are the mean values of each duplicate. No-adherent plate pellets were collected at 72 hours. Adherent plate pellets were collected at 96 hours.

### Analysis of zonulin expression in neurospheres

Neurosphere pellets were collected at 72 hours (no-adherent plates) and 96 hours (adherent plates) to analyse zonulin protein expression by WB.

Zonulin expression increased in cells cultured in NSCM than in the control ones (SM), either in no-adherent or adherent plates. In addition, zonulin resulted less expressed if NSCM was progressively added, than if it was replaced all at once (**figure 12**).

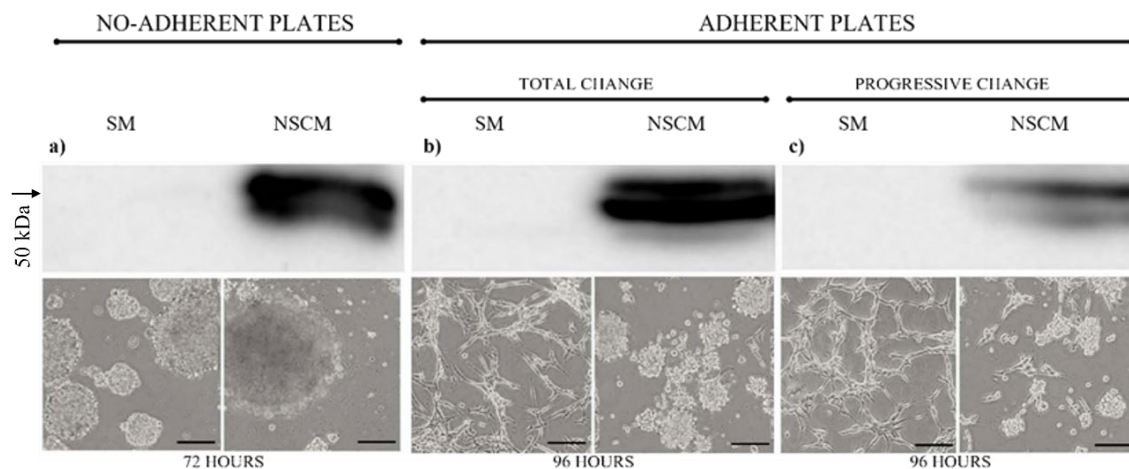


**Figure 12.** Zonulin western blot images combined with the corresponding microscope pictures (10X magnification). Scale bar: 50  $\mu$ m. SM: standard medium. NSCM: neural stem cell medium. Zonulin band corresponds to a molecular weight of approximately 50 kDa (all double band was quantified). **a)** Cells cultured in no-adherent plates in SM or in NSCM. SM: undetectable zonulin expression. NSCM: zonulin is expressed. Samples and data collected at 72 hours. **b)** Cells cultured in adherent plates, with total change of medium every 48 hours, in SM or NSCM. SM: undetectable zonulin expression. NSCM: zonulin is expressed. Samples and data collected at 96 hours. **c)** Cells cultured in adherent plates with a progressive change of medium (1/3) every 24 hours, in SM or NSCM. SM: undetectable zonulin expression. NSCM: zonulin is expressed, although at a less amount than the previous condition. Samples and data collected at 96 hours.

An overview on zonulin expression in neurospheres under different conditions is represented in **figure 13** (no statistical analysis, group size: n=2).

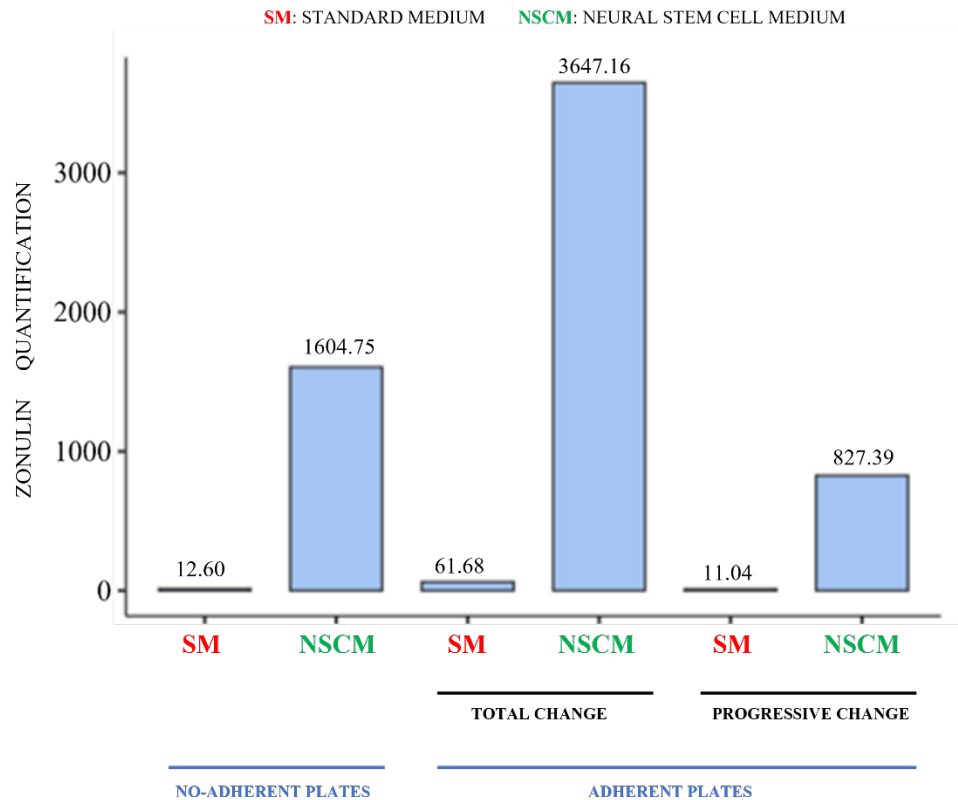


**Figure 13.** Zonulin expression in neurospheres. Histogram representing zonulin relative quantification (WB) of neurospheres, cultured in no-adherent or adherent plates, either in standard medium (SM) or neural stem cell medium (NSCM). For adherent plates, a total or progressive change of medium was performed. Quantification data reported in the graph are the mean values of each duplicate.

### Comparison of zonulin expression among tumour samples, glioma cell lines and neurospheres

All values of zonulin expression in neurospheres were gathered into a single “neurosphere” group (n=6). Then, zonulin expression was compared among tumour samples, U-87MG cells, U-118MG cells, and neurospheres. In both glioma

cell lines zonulin resulted less expressed than in neurospheres, with an overall  $p=0.010$  (figure 14).

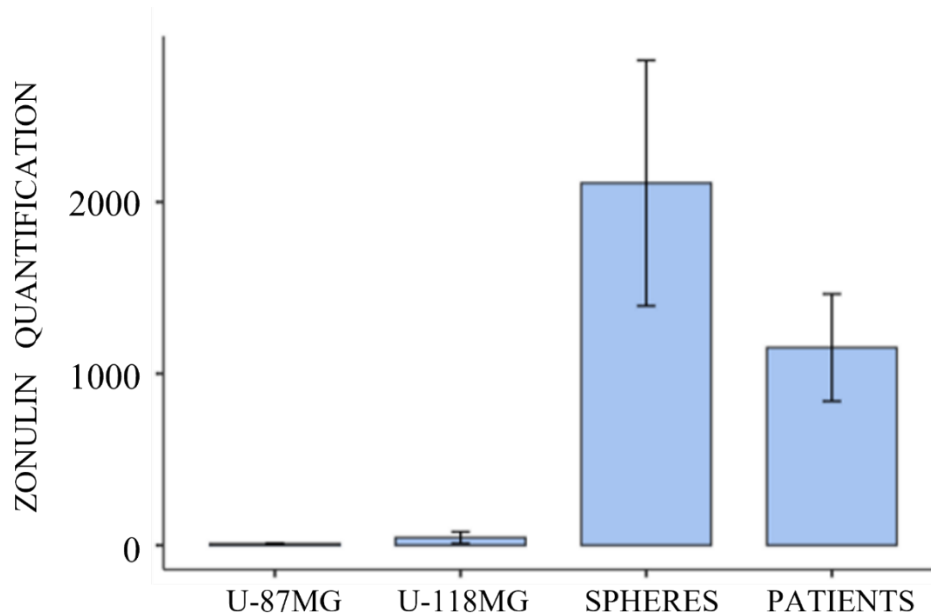


**Figure 14.** Comparison of zonulin expression among patients, GB cell lines and neurospheres. Bar plot representing zonulin relative quantification (WB) among all the groups. Overall  $p=0.010$  (Kruskal-Wallis no-parametric test). Bars show variation around the median value. U-87MG, U-118MG:  $n=10$ . Spheres:  $n=6$ . Patients:  $n=21$ .

## DISCUSSION

The present study was aimed to better characterize the role of zonulin in some crucial clinical and molecular aspects of glioblastoma (GB), as cerebral oedema, progression-free survival (PFS), and the implication of glioma stem cells (GSCs). Therefore, zonulin expression was assessed in GB patients (tissue and serum samples), in glioma cell lines U-87MG and U-118MG and in GSCs (neurospheres) obtained *in vitro* from de-differentiation of parental U-87MG cell line. Then, possible correlations between zonulin expression and clinical parameters were analysed, and zonulin expression was also compared among groups. In serum, zonulin resulted significantly correlated with a worse prognosis (lower PFS). In tumour samples, zonulin was correlated with oedema volume and contrast enhancement volume. Moreover, zonulin expression in tumour samples was at an intermediate level between GSCs *in vitro* (highest level) and glioma cell lines (lower level).

Zonulin is a recently discovered molecule, mostly studied in the alteration of intestinal barrier<sup>12</sup>. Upon translation, it is usually processed into haptoglobin (HP) to exert different functions<sup>14</sup>, but it can also keep its native structure under certain stimuli<sup>13</sup>. Most pathways involved in zonulin modulation, especially in the brain, remain unknown. Moreover, which cells express zonulin in a constitutive or inducible way are still to determine.

### **Zonulin expression in cell lines increased in stemness conditions**

In glioma cell lines U-87MG and U-118MG, cultured in standard medium (SM), zonulin was expressed. Moreover, in the present study the pattern of zonulin cellular localization was described for the first time.

After zonulin immunolabeling in U-87MG and U-118MG cell lines, a spot clustering located in nuclei was revealed. The reasons of this location are unknown and deserve further investigation.



Interestingly, when U-87MG were exposed to stem cell conditions (an artificial medium enriched with growth factors and appropriate supplements-NSCM), cells grew as neurospheres and began to strongly increment zonulin protein expression. Specifically, zonulin overexpression appeared to be linked to the medium, not to the spheric phenotype: in fact, in no-adherent plates, where a spheric shape was observable both in SM and NSCM conditions, zonulin resulted increased only in the latter condition. However, zonulin expression was higher in neurospheres submitted to a total change of medium compared to a progressive one. All together, these observations may suggest an alternative regulation pathway for zonulin expression, differently from those previously reported in literature (inflammation)<sup>13</sup>.

Positivity for CD133 detected in neurospheres allowed to identify them as GSCs. An increase in CD133 expression was detectable in GSCs that underwent a progressive renewal of NSCM, compared to those that received NSCM all at once. This event may be explained considering that CD133 expression may be regulated by gradual changes in surrounding microenvironment, even though a higher sample size is required to assess this finding. Conversely, in “progressive” condition, zonulin was less expressed than the “total” one. Moreover, GSCs cultured in the “progressive” condition showed a higher level of cellular debris, which may represent a restricting growth feature comparable to hypoxia. Previously, CD133 was found to be overexpressed in hypoxia conditions<sup>27,28</sup>.

### **Tumour samples showed an intermediate expression of zonulin compared to glioma cell lines and neurospheres.**

Zonulin expression was detected in GB tumour samples and quantified for the first time. In some cases, zonulin was detected as a double band around its expected molecular weight (50 kDa), due to its possible glycosylation<sup>9</sup>. The overall comparison of zonulin expression among tumour samples, U-87MG, U-118MG and neurospheres resulted in the following pattern: higher levels of zonulin in

neurospheres were found, compared both to patients, who placed at an intermediate level, and to GB cell lines expressing, instead, the lowest amounts of zonulin (overall  $p=0.010$ ).

As hypothesized, in tumour samples a higher level of zonulin expression was found, compared to glioma cell lines, possibly due to the microenvironment contribution. Possibly for the same reason, GSCs *in vitro* showed more elevated zonulin production compared to tumour samples and glioma cell lines: in fact, in the tumoral context, GSCs are present and modulation networks are involved. Although there is not knowledge about specific zonulin cellular expression and regulation, GSCs may be considered a possible candidate as zonulin-expressing cell pool.

As observed *in vitro*, one of zonulin modulators may be any stemness factor present in the medium. However, bigger comprehensive studies are required to demonstrate the relationship between zonulin expression and stemness factors. Spatial phenotyping, a recent well-established mapping technique that allows to localize a target molecule at single-cell level, would be a powerful tool to investigate zonulin expression inside the extremely heterogeneous GB context<sup>29</sup>.

### **Zonulin expression in patients was associated with clinical features**

Regarding clinical parameters, higher serum levels of zonulin were significantly related to worse survival outcomes, whereas only a (no significant) trend was detected for tumour samples, indicating that zonulin in serum may come from other tissues (e.g., intestine).

In tumour samples, higher levels of zonulin were significantly correlated to bigger oedema volume and contrast enhancement volume. These two clinical features are BBB impairment and neo-angiogenesis indicators. Knowing that PAR-2 receptor, a main component of zonulin signalling, is overexpressed in GB vasculature in hypoxia-driven angiogenesis<sup>30</sup>, the hypothesis of the implication of

zonulin in BBB dysfunction and tumour progression may be confirmed, although a bigger sample size would be needed to strengthen this data.

However, the present study not only provided a quantitative information of zonulin expression in GB tissue, but also correlated it to clinical parameters. In fact, till now, only a qualitative analysis of zonulin was carried out by immunostaining in high-grade glioma tissues<sup>18</sup>.

### **Future perspectives**

Preliminary data observed in this study allowed to clarify a possible implication of zonulin in important aspects of GB and may represent a base for further investigation.

To improve zonulin analysis, other housekeeping genes for mRNA normalization or a monoclonal antibody for protein detection may be used.

A further step towards zonulin analysis in GSCs, would be to isolate this cell pool from GB samples and to assess zonulin expression in it. In addition, to better understand medium contribution to stemness, would be useful to analyse zonulin expression at different time points during neurosphere formation or to perform functional assays (e.g., adding cytokines or treatment to the medium). Also, zonulin immunostaining in GSCs should be realized, to investigate its location in this specific cell pool. In tumour samples, spatial phenotyping would be a powerful tool to investigate whether other cells may express zonulin.

Circulating zonulin is being currently investigated in gastrointestinal and liver alterations as a potential promising marker<sup>19</sup>. However, it would not be a GB specific indicator, although it may be further investigated to assess possible variations due to treatment or recurrences. Moreover, genetic sequencing would be helping to understand its origin, since that N-terminal domain is tissue-specific<sup>17</sup>.

## CONCLUSIONS

The present work contributed to clarify some aspects on the role of zonulin in GB biology, providing additional information on its role in BBB impairment and tumour progression.

Main conclusions are:

1. High levels of zonulin are associated with some clinical parameters, as oedema volume, contrast enhancement volume and survival outcomes.
2. In patients zonulin is more expressed than in glioma cell lines, suggesting the influence of modulating factors in tumour microenvironment.
3. Glioma cell line U-87MG moderately express zonulin in physiological conditions, while starts producing higher amounts of zonulin if surrounding medium is enriched of stemness inducing factors.
4. GSCs *in vitro* express high levels of zonulin.

## BIBLIOGRAPHY

---

- <sup>1</sup> Kenneth Aldape et al., ‘Glioblastoma: Pathology, Molecular Mechanisms and Markers’, *Acta Neuropathologica* 129, no. 6 (June 2015): 829–48, <https://doi.org/10.1007/s00401-015-1432-1>.
- <sup>2</sup> Kayla J. Wolf et al., ‘Dissecting and Rebuilding the Glioblastoma Microenvironment with Engineered Materials’, *Nature Reviews Materials* 4, no. 10 (16 August 2019): 651–68, <https://doi.org/10.1038/s41578-019-0135-y>.
- <sup>3</sup> Michael Weller et al., ‘EANO Guidelines on the Diagnosis and Treatment of Diffuse Gliomas of Adulthood’, *Nature Reviews Clinical Oncology* 18, no. 3 (March 2021): 170–86, <https://doi.org/10.1038/s41571-020-00447-z>.
- <sup>4</sup> Milena Cankovic et al., ‘The Role of MGMT Testing in Clinical Practice’, *The Journal of Molecular Diagnostics* 15, no. 5 (September 2013): 539–55, <https://doi.org/10.1016/j.jmoldx.2013.05.011>.
- <sup>5</sup> Wolf et al., ‘Dissecting and Rebuilding the Glioblastoma Microenvironment with Engineered Materials’.
- <sup>6</sup> Zhihong Chen and Dolores Hambarzumyan, ‘Immune Microenvironment in Glioblastoma Subtypes’, *Frontiers in Immunology* 9 (8 May 2018): 1004, <https://doi.org/10.3389/fimmu.2018.01004>.
- <sup>7</sup> Mario L. Suvà and Itay Tirosh, ‘The Glioma Stem Cell Model in the Era of Single-Cell Genomics’, *Cancer Cell* 37, no. 5 (May 2020): 630–36, <https://doi.org/10.1016/j.ccell.2020.04.001>.
- <sup>8</sup> Mark Dapash et al., ‘The Interplay between Glioblastoma and Its Microenvironment’, *Cells* 10, no. 9 (31 August 2021): 2257, <https://doi.org/10.3390/cells10092257>.
- <sup>9</sup> Xiaohui Li et al., ‘Suppression of Angiotensin-(1–7) on the Disruption of Blood-Brain Barrier in Rat of Brain Glioma’, *Pathology & Oncology Research* 25, no. 1 (January 2019): 429–35, <https://doi.org/10.1007/s12253-018-0471-z>.
- <sup>10</sup> ‘Interventions to Reduce Neurological Symptoms in Patients with GBM Receiving Radiotherapy: From Theory to Clinical Practice’, *Anticancer Research* 38, no. 4 (28 March 2018), <https://doi.org/10.21873/anticancer.12494>.
- <sup>11</sup> Alessio Fasano, ‘Regulation of Intercellular Tight Junctions by Zonula Occludens Toxin and Its Eukaryotic Analogue Zonulin’, *Annals of the New York Academy of*

---

*Sciences* 915, no. 1 (25 January 2006): 214–22, <https://doi.org/10.1111/j.1749-6632.2000.tb05244.x>.

<sup>12</sup> Richard Daneman and Maria Rescigno, ‘The Gut Immune Barrier and the Blood-Brain Barrier: Are They So Different?’, *Immunity* 31, no. 5 (November 2009): 722–35, <https://doi.org/10.1016/j.immuni.2009.09.012>.

<sup>13</sup> Alessandra Di Masi et al., ‘Haptoglobin: From Hemoglobin Scavenging to Human Health’, *Molecular Aspects of Medicine* 73 (June 2020): 100851, <https://doi.org/10.1016/j.mam.2020.100851>.

<sup>14</sup> Alessio Fasano, ‘Zonulin and Its Regulation of Intestinal Barrier Function: The Biological Door to Inflammation, Autoimmunity, and Cancer’, *Physiological Reviews* 91, no. 1 (January 2011): 151–75, <https://doi.org/10.1152/physrev.00003.2008>.

<sup>15</sup> Zhixiang Wang, ‘Transactivation of Epidermal Growth Factor Receptor by G Protein-Coupled Receptors: Recent Progress, Challenges and Future Research’, *International Journal of Molecular Sciences* 17, no. 1 (12 January 2016): 95, <https://doi.org/10.3390/ijms17010095>.

<sup>16</sup> R. Lu et al., ‘Affinity Purification and Partial Characterization of the Zonulin/Zonula Occludens Toxin (Zot) Receptor from Human Brain’, *Journal of Neurochemistry* 74, no. 1 (25 December 2001): 320–26, <https://doi.org/10.1046/j.1471-4159.2000.0740320.x>.

<sup>17</sup> Durairaj Mohan Kumar et al., ‘Proteomic Identification of Haptoglobin A2 as a Glioblastoma Serum Biomarker: Implications in Cancer Cell Migration and Tumor Growth’, *Journal of Proteome Research* 9, no. 11 (5 November 2010): 5557–67, <https://doi.org/10.1021/pr1001737>.

<sup>18</sup> Marco Skardelly et al., ‘Expression of Zonulin, c-Kit, and Glial Fibrillary Acidic Protein in Human Gliomas’, *Translational Oncology* 2, no. 3 (September 2009): 117–20, <https://doi.org/10.1593/tlo.09115>.

<sup>19</sup> Mónica Díaz-Coránguez et al., ‘Transmigration of Neural Stem Cells across the Blood Brain Barrier Induced by Glioma Cells’, ed. Joseph Najbauer, *PLoS ONE* 8, no. 4 (5 April 2013): e60655, <https://doi.org/10.1371/journal.pone.0060655>.

<sup>20</sup> Charlotte M. Stuart et al., ‘Zonulin and Blood–Brain Barrier Permeability Are Dissociated in Humans’, *Clinical and Translational Medicine* 12, no. 7 (July 2022), <https://doi.org/10.1002/ctm2.965>.

<sup>21</sup> David J. Sanchez et al., ‘Haptoglobin Gene Expression in Human Glioblastoma Cell Lines’, *Neuroscience Letters* 303, no. 3 (May 2001): 181–84, [https://doi.org/10.1016/S0304-3940\(01\)01748-7](https://doi.org/10.1016/S0304-3940(01)01748-7).

- 
- <sup>22</sup> Fortunata Iacopino et al., ‘Isolation of Cancer Stem Cells from Three Human Glioblastoma Cell Lines: Characterization of Two Selected Clones’, ed. Giovanni Camussi, *PLoS ONE* 9, no. 8 (14 August 2014): e105166, <https://doi.org/10.1371/journal.pone.0105166>.
- <sup>23</sup> Shi-cang Yu et al., ‘Isolation and Characterization of Cancer Stem Cells from a Human Glioblastoma Cell Line U87’, *Cancer Letters* 265, no. 1 (June 2008): 124–34, <https://doi.org/10.1016/j.canlet.2008.02.010>.
- <sup>24</sup> Hemamylammal Sivakumar et al., ‘Multi-Cell Type Glioblastoma Tumor Spheroids for Evaluating Sub-Population-Specific Drug Response’, *Frontiers in Bioengineering and Biotechnology* 8 (15 September 2020): 538663, <https://doi.org/10.3389/fbioe.2020.538663>.
- <sup>25</sup> Nicholas Silver et al., ‘Selection of Housekeeping Genes for Gene Expression Studies in Human Reticulocytes Using Real-Time PCR’, *BMC Molecular Biology* 7, no. 1 (December 2006): 33, <https://doi.org/10.1186/1471-2199-7-33>.
- <sup>26</sup> Sheila K. Singh et al., ‘Identification of Human Brain Tumour Initiating Cells’, *Nature* 432, no. 7015 (November 2004): 396–401, <https://doi.org/10.1038/nature03128>.
- <sup>27</sup> Kun Liu et al., ‘Hypoxia-Induced GLT8D1 Promotes Glioma Stem Cell Maintenance by Inhibiting CD133 Degradation through N-Linked Glycosylation’, *Cell Death & Differentiation* 29, no. 9 (September 2022): 1834–49, <https://doi.org/10.1038/s41418-022-00969-2>.
- <sup>28</sup> A Soeda et al., ‘Hypoxia Promotes Expansion of the CD133-Positive Glioma Stem Cells through Activation of HIF-1 $\alpha$ ’, *Oncogene* 28, no. 45 (12 November 2009): 3949–59, <https://doi.org/10.1038/onc.2009.252>.
- <sup>29</sup> Mark Sorin et al., ‘Single-Cell Spatial Landscapes of the Lung Tumour Immune Microenvironment’, *Nature* 614, no. 7948 (16 February 2023): 548–54, <https://doi.org/10.1038/s41586-022-05672-3>.
- <sup>30</sup> Katrin J. Svensson et al., ‘Hypoxia Triggers a Proangiogenic Pathway Involving Cancer Cell Microvesicles and PAR-2–Mediated Heparin-Binding EGF Signaling in Endothelial Cells’, *Proceedings of the National Academy of Sciences* 108, no. 32 (9 August 2011): 13147–52, <https://doi.org/10.1073/pnas.1104261108>.